Article

Selective Monitoring and Imaging of Eosinophil Peroxidase Activity with a J-Aggregating Probe

Tae-Il Kim, Byunghee Hwang, Boeun Lee, Jeehyeon Bae, and Youngmi Kim

J. Am. Chem. Soc., **Just Accepted Manuscript** • Publication Date (Web): 29 Aug 2018

Selective Monitoring and Imaging of Eosinophil Peroxidase Activity with a J-Aggregating Probe

Tae-Il Kim,[†,⊥] Byunghee Hwang,[†,⊥] Boeun Lee,[‡,⊥] Jeehyeon Bae,*[,§] and Youngmi Kim*[,†]

[†]Department of Chemistry and Research Institute of Basic Sciences, Kyung Hee University, 26 Kyungheedae-ro, Dongdaemun-gu, Seoul 02447, Korea

[‡]Department of Life Science, Chung-Ang University, 84 Heukseok-ro, Dongjak-gu, Seoul 06974, Korea

[§]School of Pharmacy, Chung-Ang University, 84 Heukseok-ro, Dongjak-gu, Seoul 06974, Korea

ABSTRACT: The specific detection of eosinophil peroxidase (EPO) activity requires the difficult distinction between hypobromous acid generated by EPO and hypochlorous acid generated by other haloperoxidases. Here we report a fluorogenic probe that is halogenated with high kinetic selectivity (≥1200:1) for HOBr over HOCl. Heavy atom effects do not quench the dibrominated product because of its self-assembly into emissive J-aggregates that provide a turn-on signal. Applications of this fluorogen to EPO activity assays, dip-stick sensors, fluorescence imaging of EPO activity, assays of oxidative stress in cancer cells, and immune response detection in live mice are reported.

INTRODUCTION

Eosinophils are granulocytic leukocytes that play critical roles in host defense against infections, and are involved in the pathogenesis of asthma and allergic diseases.[1,2] Moreover, numerous disorders, from autoimmune diseases to Hodgkin's lymphoma have been associated with abnormally elevated eosinophil counts.[3,4] The cytotoxic activity of granulocytes relies in part on their ability to generate toxic reactive oxygen species (ROS), via haloperoxidases that oxidize halides (X^-) to hypohalous acids (HOX) using hydrogen peroxide.[5-9] Myeloperoxidase (MPO), found in neutrophils, mainly converts Cl^- to hypochlorous acid (HOCl, pK_a 7.6).[10,11] Eosinophil peroxidase (EPO) instead preferentially oxidizes Br^- to hypobromorous acid (HOBr, pK_a 8.8) despite the 1000-fold excess of Cl^- over Br^- ([Cl^-] 100-140 mM, [Br^-] 20-100 μM).[12] The strong oxidizing and halogenating ability of HOBr contributes to inflammation and tissue damage resulting from eosinophilic disorders.[5-7]

No fluorescent probe for the specific detection of EPO activity is currently available. Tremendous strides have been made in the development of chemically reactive fluorescent probes for the selective detection and imaging of H_2O_2, or HOCl (and hence MPO activity),[13-18] but the design of probes to specifically detect HOBr generated by EPO faces important challenges.[19-21] HOCl is a more powerful oxidizing agent than HOBr, which, given their similar chemistry, precludes a selective redox-triggered signal.[22] Other ROS (e.g. H_2O_2, $ONOO^-$, $\cdot O_2^-$) are also known interferences in some redox-based detection schemes.[23-26] Indeed, these are issues with the most popular commercially available fluorescent probe for monitoring EPO activity, aminophenyl fluorescein (APF, Scheme 1a).[27] Though able to detect EPO activity, APF also responds to MPO-generated HOCl, and other ROS such as the hydroxyl radical (·OH) or peroxynitrite ($ONOO^-$), often with higher sensitivity.[28,29] The electrophilic halogenation of alkenes or electron-rich aromatic substrates does show appreciable kinetic selectivity for HOBr over HOCl (up to 10^4:1 for Tyr residues).[30,31] However, the resulting brominated derivatives are typically quenched in solution due to heavy atom effects that increase intersystem crossing and non-radiative deactivation rates, making this halogenation approach unappealing for the development of fluorescent probes.[32-34]

Scheme 1. Schematic illustration of the design of fluorescent "turn-on" probes for the detection of EPO activity.

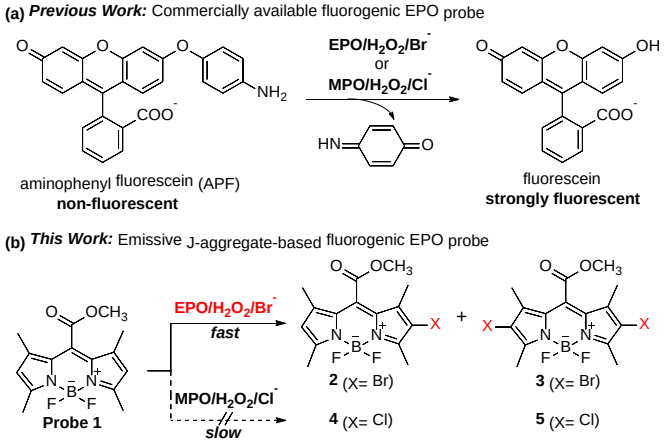

In this paper, we describe the use of BODIPY chromophores that form J-aggregates to solve the HOX selectivity conundrum in the detection of EPO activity. Probe **1** is rapidly dibrominated with EPO-generated HOBr with a high kinetic selectivity over its chlorination with HOCl (Scheme 1b). The resulting **3** does not suffer from poor photophysical properties associated with brominated chromophores; on the contrary, it self-assembles into highly emissive red-shifted J-aggregates to result in a clean turn-on fluorescence signal. Using this probe, the selective detection, assaying and imaging of HOBr generation by EPO without interference from MPO-generated HOCl are for the first time demonstrated.

RESULTS AND DISCUSSION

Synthesis. Probe **1** was prepared according to literature procedures.[35] To confirm the feasibility of the proposed sensing Scheme 1b, the expected products of the electrophilic bromination of **1** with HOBr, **2** and **3**, were independently synthesized (Scheme S1).

Photophysical Property and Self-Assembly Studies. All *meso*-ester-substituted-BODIPYs **1–3** have low solution emission quantum yields in solution (Φ_F in CH_3CN = 0.003 (**1**); 0.004 (**2**); 0.002 (**3**); Table S1), as expected for sterically congested, *meso*-substituted 1,3,5,7-tetramethyl BODIPYs.[35] Probe **1** was previously shown to display aggregation-induced emission enhancement (AIEE) features through J-aggregation,[35] evidenced by a large red-shift from 509 to 581 nm upon aggregation, a small Stokes shift (176 cm^{-1}), a narrow emission band (FWHM = 560 cm^{-1}), an increased fluorescence rate constant (from the k_F = 3.3 x 10^7 s^{-1} in solution to 4.4 x 10^8 s^{-1} in suspended aggregates), and a head-to-tail arrangement of its transition dipoles (displacement angle θ < 54.7°; 33° for **1**).

The suspended colloidal aggregates of dibromo-BODIPY **3** (20 μM) in CH_3CN–water mixtures ($f_w \geq$ 90%; 540 ± 10 nm by DLS, Figure 1b) display the same spectroscopic features consistent with J-aggregate formation among *meso*-substituted 1,3,5,7-tetramethyl BODIPYs.[35,36] Its absorption maximum shifts from 539 nm in CH_3CN solution to 619 nm in CH_3CN–water mixtures (Figure S8). Its fluorescence emission features a small Stokes shift (52 cm^{-1}), a narrow emission band (FWHM = 724 cm^{-1}), a 6.3-fold increase in fluorescence rate constant (k_F (sol) = 1.1 × 10^7 s^{-1}; k_F (agg) = 6.9 × 10^7 s^{-1}; Figure S20). The characteristic spectroscopic features of J-aggregates were seen in concentrations of **3** as low as *ca.* 0.25 μM (Figure S9).

Importantly for a clean turn-on signal, the red emissive (621 nm) aggregates of dibrominated **3** are fully resolved from the parent probe **1**, which self-assembles into orange emissive J-aggregates showing a sharp emission band at 581 nm (Figures S2-S3 and Figure 2b). Moreover, aggregates of the monobrominated BODIPY **2** in the same CH_3CN–water mixtures ($f_w \geq$ 90%) do not interfere, displaying absorption and emission maxima at *ca.* 567 nm and 580 nm, respectively (Figures S5-S6).

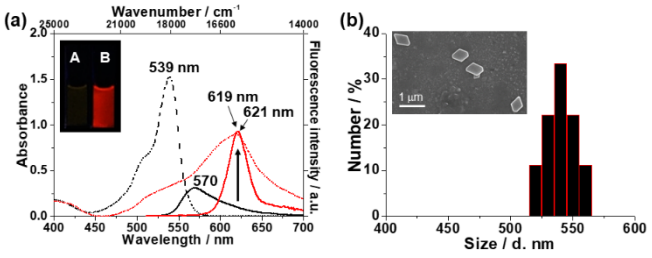

Figure 1. (a) Absorption (dotted lines) and emission (solid lines) spectra of **3** (20 μM) in CH_3CN (black) and 0.1:99.9 (v/v) CH_3CN:H_2O (red, 100 mM acetate buffer, pH 5.0). λ_{ex} = 480 nm. Insets: Photographs of each solution (A: CH_3CN, B: CH_3CN/H_2O = 0.1:99.9 (v/v)) under irradiation at 365 nm. (b) Size distribution of aggregates of **3** by DLS (540 ± 10 nm). Inset: SEM images (490 ± 30 nm) of aggregates of **3**. [**3**] = 20 μM.

HOBr Sensing in Solution. The sensory response of probe **1** toward HOBr was first evaluated in aqueous solution (100 mM acetate buffer, pH 5.0, 0.1% CH_3CN) at 25 °C (Figure 2, and Figures S21-22). Upon addition of HOBr, the absorption and emission peaks of **1** decrease markedly, while the characteristic red-shifted absorption and emission bands of the suspended aggregates of **3** emerge instantly. To the naked eye, these correspond to a change from pink to purple (Figure 2a, inset), and under handheld UV lamp irradiation (365 nm) to a change from orange to red (Figure 2b, inset). Time course studies revealed that the fluorescence turn-on process is fast (≤ 2s; Figure S23), and HPLC–MS analysis of the reaction mixture confirmed the formation of **3** as a major product (Figure S39).

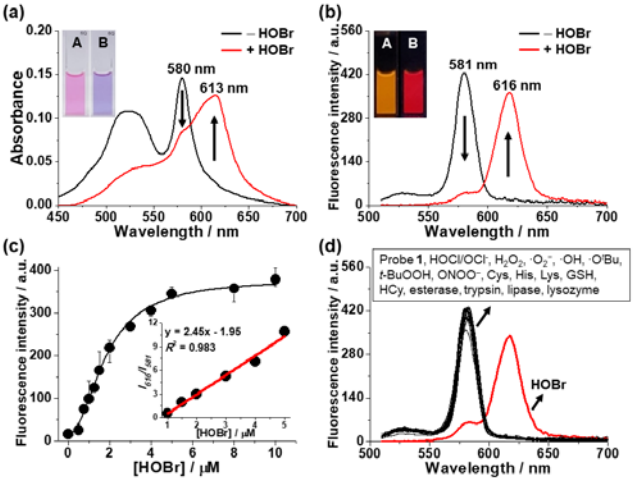

Figure 2. Absorption (a) and fluorescence (b) spectra of the self-assembled **1** (2.5 μM) before (black) and immediately (≤ 2s) after (red) addition of HOBr (10 μM). Insets: Photographs of **1** (20 μM) before (A) and after (B) the addition of HOBr (40 μM) under ambient light (a) and UV light (b). (c) Fluorescence intensity at 616 nm as a function of [HOBr] (0–10 μM). Inset: Ratiometric (I_{616}/I_{581}) calibration curve. (d) Fluorescence spectra of probe **1** (2.5 μM) in the presence of various biologically relevant species (5 μM HOBr, 50 μM for other ROS, 1 mM for amino acids and biothiols, and 1 mg/mL for others). All spectra were obtained immediately after addition of each analyte to **1** in acetate buffer (100 mM, pH 5.0, 0.1% CH_3CN) at 25 °C. λ_{ex} = 480 nm.

As shown in Figure 2c, the fluorescence intensity at 616 nm increases rapidly with increasing HOBr concentration within the measured range (0–10 μM), levelling off after the addition of 2 equivalents of HOBr with *ca.* 22-fold increase in fluorescence intensity at 616 nm (Figure S22). A linear relationship exists between the ratio of the emission intensities (I_{616}/I_{581}) and the concentration of HOBr in the range of 1–5 μM (R^2 = 0.983) (Figure 2c, inset). The detection limit (3σ/slope) for HOBr using probe **1** was determined to be 3.8 nM (Figure S24).

More importantly, the probe **1** (2.5 μM) displayed excellent selectivity toward HOBr over other biologically relevant molecules (Figure 2d). Among reactive oxygen species (ROS), only HOBr promotes a dramatic enhancement in emission at 616 nm; no significant change in the emission spectra of **1** occurs in the presence of HOCl/OCl^-, H_2O_2, superoxide ($\cdot O_2^-$), hydroxyl (·OH) or *tert*-butoxy radicals ($\cdot O^tBu$), *tert*-butyl hydroperoxide (*t*-BuOOH), or peroxynitrite ($ONOO^-$), even at higher concentrations (5 μM for HOBr and 50 μM for others). Probe **1** can react with a large excess of HOCl/OCl^- (≥ 200

μM) to give the dichlorinated product **5** (Figures S26 and S40). However, the chlorination reaction is not kinetically competitive with the bromination reaction. HPLC−MS analysis confirmed that the reaction of probe **1** (2.5 μM) in the presence of both HOBr (12.5 μM) and HOCl (up to 400 μM) only lead to the formation of **3** (Figure S41). Furthermore, in the absence of any HOBr, false positive responses elicited by HOCl do not take place within biologically relevant concentrations ([HOCl] ≤ 100 μM; Figures S26-S27).[37-39] The robustness of this assay against the interference of HOCl/OCl^- results from a 1200-fold kinetic selectivity for HOBr over HOCl in the halogenation reactions of the BODIPY dye (Figure S28).[40]

In addition, probe **1** is not affected by the presence of amino acids with nucleophilic side chains (Cys, His, Lys), biothiols (GSH, HCy), or common hydrolytic enzymes (esterase, trypsin, lipase, lysozyme). (Figure 2d). Moreover, the self-assembled J-aggregates of both **1** and **3** remained stable in the presence of proteins (myoglobin, hemoglobin, bovine serum albumin) and lipids (cholesterol, oleic acid, phosphatidylcholine) (Figure S16), and in a pH range from 4 to 9 (Figure S17). The fluorescence response of probe **1** toward HOBr is nevertheless pH-dependent. The greater response under acidic conditions (pH < 6) is consistent with the proposed electrophilic halogenation pathway (Figure S25).

EPO Activity Assays in Solution. Incubation of **1** (2.5 μM) with EPO (0.5–150 ng/mL) in acetate buffer solution (100 mM, pH 5.0, 50 μM H_2O_2, 100 μM KBr, 0.1% CH_3CN) at 25 °C resulted in spectral changes consistent with the formation of emissive J-aggregates of dibromo-BODIPY **3** (Figure 3a and 3b). The characteristic red-shifted absorption and emission bands ($\lambda_{abs.max}$ = 613 nm, $\lambda_{em.max}$ = 616 nm) grow instantly (≤ 2s, Figure S32), and the latter increases linearly (R^2 = 0.9957) with EPO concentrations ranging from 0 to 125 ng/mL (Figure 3b inset). The major reaction product was unambiguously identified as dibromo-BODIPY **3** by HPLC–MS analysis of the assay solution (Figure S42). Probe **1** can detect EPO activity as low as 0.09 ng/mL (3σ/slope, Figure 3b inset and Figure S33), which is much lower than the median EPO serum levels of either healthy subjects (7.2 ng/mL) or severely asthmatic patients (22.9 ng/mL).[41,42] The generation of **3** was optimal at pH 5, but there was substantial production of **3** even at pH 7.4 (Figure S35).

The enhancement of fluorescence intensity at 616 nm was suppressed in a dose-dependent manner in the presence of a known EPO inhibitor, 4,4'-diaminodiphenylsulfone (dapsone) (Figure S37)[43] or the HOBr scavenger *N*-acetyl-cysteine (NAC) (Figure S38).[44] These results confirm that the formation of **3** is driven by EPO-dependent HOBr generation.

Control experiments established that a positive response is only observed in the simultaneous presence of EPO, Br^-, and H_2O_2 in the analytical sample (Figure 3c). The HOCl-generating combination of MPO, H_2O_2 and Cl^- system did not elicit a response from probe **1** (entry 7); nevertheless, their presence did not interfere with the EPO activity assay (entries 9-10). Considering the similarities between the structures and functions EPO and MPO, and that of their respective outputs HOBr and HOCl, the selective detection of EPO over MPO with **1** is notable. To our knowledge, probe **1** is the first small molecule fluorescent "turn-on" probe that can selectively detect EPO activity over that of MPO.

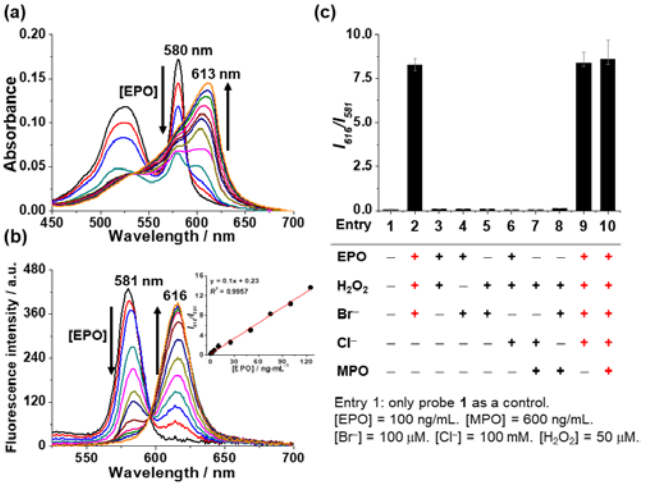

Figure 3. Absorption (a) and fluorescence (b) spectra of the self-assembled **1** upon treatment with EPO (0–150 ng/mL) in 100 mM acetate buffer (pH 5.0, 0.1% CH_3CN, 25 °C) containing 50 μM H_2O_2 and 100 μM KBr. Inset: Ratiometric (I_{616}/I_{581}) calibration curve ([EPO]: 0–125 ng/mL). (c) Fluorescence response (I_{616}/I_{581}) of probe **1** in various conditions. All spectra were obtained immediately after addition of **1** to each assay solution, and fluorescence intensities at 581 nm and 616 nm were recorded. [**1**] = 2.5 μM. λ_{ex} = 480 nm.

Dip-Stick Sensors. The EPO activity assay could finally be simplified by taking advantage of bright emission of the aggregates of **1** and **3** in the solid-state. As shown in Figure 4, paper strips coated with **1** can be used as 'dip-sticks' to estimate the concentration of EPO in aqueous samples. The availability of simplified and rapid EPO assays is especially appealing for point-of-care measurements using nasal mucus or bronchoalveolar lavage fluids in cases of allergies, asthma, or related eosinophilic disorders.[41,45]

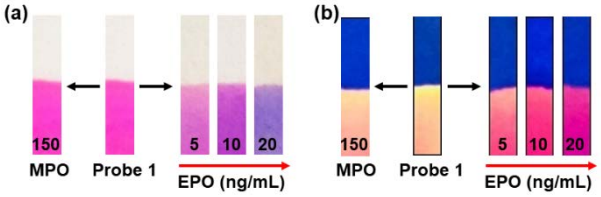

Figure 4. Photographs of color (a) and fluorescence (b) responses of probe **1**-coated paper strips following a 15 s dip in solutions of MPO/H_2O_2/Cl^- (left) or EPO/H_2O_2/Br^- (right). [Cl^-] = 100 mM, [H_2O_2] = 50 μM, [MPO] =150 ng/mL; [Br^-] = 100 μM, [H_2O_2] = 50 μM, [EPO] = 5, 10, and 20 ng/mL. The fluorescence response images were taken under UV irradiation (365 nm).

Fluorescence Imaging of HOBr Generation by EPO. Probe **1** is suitable for the confocal fluorescence imaging of EPO/H_2O_2/Br^- (HOBr) in living RAW264.7 macrophage cells, and shows no cytotoxicity up to 100 μM (Figure S46). Cells incubated with probe **1** (10 μM) alone showed strong yellow channel fluorescence (570–590 nm, λ_{ex} 488 nm), but none was observed from the red channel (600–620 nm, Figure 5a, #1-2). By contrast, upon treatment with exogenous EPO/H_2O_2/Br^-, red channel luminescence increased as the signals for the yellow channel diminished (Figure 5a, #6-7) within the cells in proportion to the added EPO (Figure S47). The red fluores-

cence signal was observed within 10 min and remained stable for at least 90 min (Figure S48).

In control experiments, co-treatment of the cells with the ROS scavenger *N*-acetylcysteine (NAC, Figure 5a, #17) or the EPO inhibitor dapsone (Figure S49) inhibited the response of probe **1** toward EPO/H_2O_2/Br^-. In addition, no red fluorescence was observed in the probe **1**-loaded cells incubated with MPO (up to 600 ng/mL), H_2O_2 (50 μM), and KCl (100 mM) (Figure 5a, #12, and Figure S50). Co-staining experiments with the DNA-binding dye DAPI indicate that the probe did not co-localize in the nuclei, but instead accumulated in the cytoplasm of the cells. Taken together, these results indicate that probe **1** is taken up by the macrophage cells efficiently, and that the internalized probe is selectively activated by the EPO-generated HOBr.

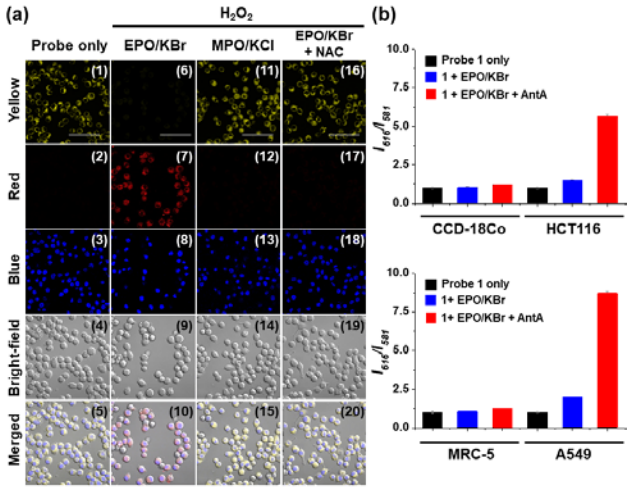

Figure 5. (a) Confocal fluorescence images of probe **1** (10 μM)-loaded living macrophage cells (RAW264.7) treated with different conditions. The cells were incubated with **1** for 30 min at 37 °C and then imaged (#1-5); **1**-loaded cells were incubated with KBr (100 μM), H_2O_2 (50 μM) and EPO (150 ng/mL) for 30 min either in the absence (#6-10) or the presence of 10 mM NAC (#16-20); **1**-loaded cells were incubated with KCl (100 mM), H_2O_2 (50 μM) and MPO (600 ng/mL) for 30 min (#11-15). The cells were co-stained with the blue fluorescent DNA binding dye DAPI. (Top to bottom) Fluorescence images from yellow channel (Ex = 488 nm, Em = 570-590 nm), red channel (Ex = 488 nm, Em = 600-620 nm), blue channel (Ex = 405 nm, Em = 400–520 nm), bright-field, and merged images from the four channels. (b) Comparative fluorescence intensity ratios (I_{616}/I_{581}) of probe **1** measured using a multi-plate reader in cancer (HCT116, A549), normal (CCD-18Co, MRC-5), and AntA-stimulated (red) cell lysates, before (black) and after (blue) conversion of H_2O_2 by EPO/KBr.

Fluorescence Assays of Oxidative Stress in Cancer Cells. Cancer cells are under increased oxidative stress due to altered metabolic activity and mitochondrial dysfunction, resulting in higher steady-state H_2O_2 levels compared to normal cells.[46,47] Although probe **1** does not respond to H_2O_2, its catalytic conversion to HOBr by EPO/Br^- elicits a response that is sufficiently sensitive to discriminate between the oxidative stress levels found in cancer and normal cells (Figure 5b). The fluorescence response (I_{616}/I_{581}) was measured in human colon and lung cancer cell (HCT116 and A549) lysates incubated with probe **1**, and compared with those of respective normal CCD-18Co colon cell and MRC-5 lung cell lysates (Figure 5b). In the presence of added EPO/Br^-, cancer cells lysates showed increases in fluorescence intensity ratios (I_{616}/I_{581}) by 1.5–2 fold, relative to their respective normal cells. The responses were further amplified (4–7 fold) in cancer cells sensitized to oxidative stress by the mitochondrial electron-transport-chain blocker antimycin A (AntA).[48]

Eosinophil Immune Response Detection in Live Mice. The utility of probe **1** was further extended to the detection of EPO-generated HOBr in response to a bacterial infection in a mouse model (Figure 6). Acute infection in a BALB/c mouse was induced by intraperitoneal (i.p.) injection of *Salmonella*.[49] Although the mice did not show any visible sign of disease at 72 h post-inoculation, a significant increase in the numbers of eosinophils in *Salmonella*-infected mice was confirmed (Figure 6a). The plasma and granulocytes were then separated from the whole blood, and treated with probe **1**. No noticeable increase in fluorescence intensity ratios (I_{616}/I_{581}) was observed in the plasma and granulocyte mixture obtained from uninfected mice. By contrast, a 3.5-fold increase (I_{616}/I_{581}) was observed in the samples from *Salmonella*-infected mice (Figure 6b). Probe **1**-coated paper strips could also be used to detect increased EPO activity in the same samples (Figure S52). These results demonstrate the applicability of probe **1** in the detection of eosinophil immune response elicited by early-stage bacterial infections in live mammals.

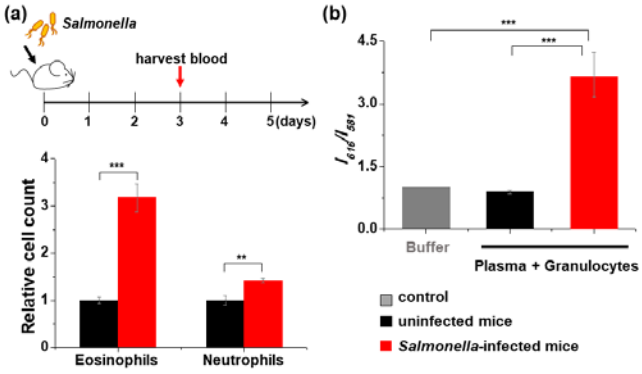

Figure 6. (a) Above: Mice experiment schedule; Below: Levels of eosinophils and neutrophils in *Salmonella*-infected mice (red bars) relative to uninfected mice as control (black bars). (b) Fluorescence response (I_{616}/I_{581}) of probe **1** (25 μM) in the absence (gray) and the presence of plasma and granulocytes from uninfected (black) and *Salmonella*-infected mice (red). The fluorescence intensity ratios (I_{616}/I_{581}) were normalized to that of uninfected mice. Five mice per group were used for analysis. $^{**}p < 0.01$, $^{***}p < 0.005$.

CONCLUSION

In summary, differences in the rates of electrophilic aromatic halogenation of probe **1**, and in the photophysical properties of the resulting halogenated BODIPY dyes (e.g. **3**) were exploited to allow for the selective detection, assaying and imaging of HOBr generation by EPO without interference from the corresponding HOCl production by MPO. The probe's response is fast (≤ 2s), highly sensitive (LOD: 0.09 ng/mL for EPO), and benefits from the advantageous photophysical properties that results from the self-assembly of both **1** and **3** in J-aggregates (narrow, non-overlapping bright emission bands). These features make probe **1** uniquely suited for investigating delicate changes in EPO activity and HOBr levels as pathological biomarkers.

ASSOCIATED CONTENT

Supporting Information

The Supporting Information is available free of charge on the ACS Publications website.

Synthetic schemes and experimental details

Additional spectroscopic data and fluorescence images

AUTHOR INFORMATION

Corresponding Authors

*E-mail: jeehyeon@cau.ac.kr. Fax: +82 2-861-7338 (J.B.).

*E-mail: youngmi.kim@khu.ac.kr. Fax: +82 2-961-0443 (Y.K.).

Author Contributions

⊥T.-I.K., B.H. and B.L. contributed equally to this work.

Notes

The authors declare no competing financial interests.

ACKNOWLEDGMENT

This research was supported by National Research Foundation of Korea (NRF) grants funded by the Korean government (MSIP) (NRF-2018R1D1A1B07044894, NRF-2017M3D9A1073769 and NRF-2015R1A5A1008958).

REFERENCES

(1) Blanchard, C.; Rothenberg, M. E. *Adv. Immunol.* **2009**, *101*, 81–121.

(2) Fulkerson, P. C.; Rothenberg, M. E. *Nat. Rev. Drug Discov.* **2013**, *12*, 117–129.

(3) Jacobsen, E. A.; Helmers, R. A.; Lee, J. J.; Lee, N. A. *Blood* **2012**, *120*, 3882–3890.

(4) Rosenberg, H. F.; Dyer, K. D.; Foster, P. S. *Nat. Rev. Immunol.* **2013**, *13*, 9–22.

(5) Weiss, S. J.; Test, S. T.; Eckmann, C. M.; Roos, D.; Regiani, S.; *Science* **1986**, *234*, 200–203.

(6) Henderson, Jr, W. R. *Peroxidases in Chemistry and Biology Vol. 1*; Everse, J.; Everse, K. E.; Grisham, M. B. Ed. CRC Press: Boca Raton, 1991; pp. 105–121.

(7) Wang, J.; Slungaard, A. *Arch. Biochem. Biophys.* **2006**, *445*, 256–260.

(8) Nicolussi, A.; Auer, M.; Sevcnikar, B.; Paumann-Page, M.; Pfanzagl, V.; Zámocký, M.; Hofbauer, S.; Furtmüller, P. G.; Obinger, C. *Arch. Biochem. Biophys.* **2018**, *643*, 14–23.

(9) Davies, M. J.; Hawkins, C. L.; Pattison, D. I.; Rees, M. D. *Antioxid. Redox Signal.* **2008**, *10*, 1199–1234.

(10) Harrison, J. E.; Shultz, J. *J. Biol. Chem.* **1976**, *251*, 1371–1374.

(11) Kettle, A. J.; Winterbourn, C. C. *Redox Rep.* **1997**, *3*, 3–15.

(12) Mayeno, A. N.; Curran, A. J.; Roberts, R. L.; Foote, C. S. *J. Biol. Chem.* **1989**, *264*, 5660–5668.

(13) Lippert, A. R.; Van de Bittner, G. C.; Chang, C. J. *Acc. Chem. Res.* **2011**, *44*, 793–804.

(14) Lou, Z.; Li, P.; Han, K. *Acc. Chem. Res.* **2015**, *48*, 1358–1368.

(15) Chen, X.; Wang, F.; Hyun, J. Y.; Wei, T.; Qiang, J.; Ren, X.; Shin, I.; Yoon, J. *Chem. Soc. Rev.* **2016**, *45*, 2976–3016.

(16) Koide, Y.; Urano, Y.; Kenmoku, S.; Kojima, H.; Nagano, T. *J. Am. Chem. Soc.* **2007**, *129*, 10324–10325.

(17) Panizzi, P.; Nahrendorf, M.; Wildgruber, M.; Waterman, P.; Figueiredo, J.-L.; Aikawa, E.; McCarthy, J.; Weissleder, R.; Hilderbrand, S. A. *J. Am. Chem. Soc.* **2009**, *131*, 15739–15744.

(18) Koide, Y.; Urano, Y.; Hanaoka, K.; Terai, T.; Nagano, T. *J. Am. Chem. Soc.* **2011**, *133*, 5680–5682.

(19) For state-of-the art probes exhibiting a degree of kinetic selectivity for HOBr over HOCl, see: Yu, F.; Song, P.; Li, P.; Wang, B.; Han, K. *Chem. Commun.* **2012**, *48*, 7735–7737.

(20) Product selectivity for HOBr over HOCl, see: Xu, K.; Luan, D.; Wang, X.; Hu, B.; Liu, X.; Kong, F.; Tang, B. *Angew. Chem., Int. Ed.* **2016**, *55*, 12751–12754, and ref 21.

(21) Liu, X.; Zheng, A.; Luan, D.; Wang, X.; Kong, F.; Tong, L.; Xu, K.; Tang, B. *Anal. Chem.* **2017**, *89*, 1787–1792.

(22) Wang, B.; Li, P.; Yu, F.; Chen, J.; Qu, Z.; Han, K. *Chem. Commun.* **2013**, *49*, 5790–5792.

(23) Xu, K.; Chen, H.; Tian, J.; Ding, B.; Xie, Y.; Qiang, M.; Tang, B. *Chem. Commun.* **2011**, *47*, 9468–9470.

(24) Liu, S.-R.; Wu, S.-P. *Org. Lett.* **2013**, *15*, 878–881.

(25) Manjare, S. T.; Kim, S.; Heo, W. D.; Churchill, D. G. *Org. Lett.* **2014**, *16*, 410–412.

(26) Qu, Z.; Ding, J.; Zhao, M.; Li, P. *J. Photochem. Photobiol. A* **2015**, *299*, 1–8.

(27) Flemmig, J.; Zschaler, J.; Remmler, J.; Arnhold, J. *J. Biol. Chem.* **2012**, *287*, 27913–27923.

(28) Setsukinai, K.; Urano, Y.; Kakinuma, K.; Majima, H. J.; Nagano, T. *J. Biol. Chem.* **2003**, *278*, 3170–3175.

(29) Gomes, A.; Fernandes, E.; Lima, J. L.F.C. *J. Biochem. Biophys. Methods* **2005**, *65*, 45–80.

(30) Pattison, D. I.; Davies, M. J. *Biochemistry* **2004**, *43*, 4799–4809.

(31) Ximenes, V. F.; Morgon, N. H.; de Souza, A. R. *J. Inorg. Biochem.* **2015**, *146*, 61–68.

(32) de Carvalho Bertozo, L.; Zeraik, M. L.; Ximenes, V. F. *Anal. Biochem.* **2017**, *532*, 29–37.

(33) Kamkaew, A.; Lim, S. H.; Lee, H. B.; Kiew, L. V.; Chung, L. Y.; Burgess, K. *Chem. Soc. Rev.* **2013**, *42*, 77–88.

(34) Zhang, X.-F.; Yang, X. *J. Phys. Chem. B* **2013**, *117*, 5533–5539.

(35) Kim, S.; Bouffard, J.; Kim, Y. *Chem. Eur. J.* **2015**, *21*, 17459–17465.

(36) Choi, S.; Bouffard, J.; Kim, Y. *Chem. Sci.* **2014**, *5*, 751–755.

(37) Palmer, L. J.; Cooper, P. R.; Ling, M. R.; Wright, H. J.; Huissoon, A.; Chapple, I. L. C. *Clin. Exp. Immunol.* **2012**, *167*, 261–268.

(38) Schraufstätter, I. U.; Browne, K.; Harris, A.; Hyslop, P. A.; Jackson, J. H.; Quehenberger, O.; Cochrane, C. G. *J. Clin. Invest.* **1990**, *85*, 554–562.

(39) Fukui, K.; Kaneda, M.; Takahashi, E.; Washio, M.; Doi, K. *J. Mol. Cell. Cardiol.* **1994**, *26*, 455–461.

(40) The higher reactivity of HOBr over HOCl in electrophilic halogenation reactions has been ascribed to its greater polarizability and weaker oxygen-halogen bond. See: (a) Voudrias, E. A.; Reinhard, M. *Environ. Sci. Technol.* **1988**, *22*, 1049−1056. (b) Sivey, J. D.; Arey, J. S.; Tentscher, P. R.; Roberts, A. L. *Environ. Sci. Technol.* **2013**, *47*, 1330−1338.

(41) Sanz, M. L.; Parra, A.; Prieto, I.; Diéguez, I.; Oehling, A. K. *Allergy* **1997**, *52*, 417–422.

(42) Krug, N.; Napp, U.; Enander, I.; Eklund, E.; Rieger, C. H. L.; Schauer, U. *Clin. Exp. Allergy* **1999**, *29*, 1507–1515.

(43) Bozeman, P. M.; Learn, D. B.; Thomas, E. L. *Biochem. Pharmacol.* **1992**, *44*, 553–563.

(44) Zafarullah, M.; Li, W. Q.; Sylvester, J.; Ahmad, M. *Cell. Mol. Life Sci.* **2003**, *60*, 6–20.

(45) Varga, S. M.; Beckman, N. A.; Chu, M.; Braciale, T. J. *J. Immunol. Methods* **2002**, *262*, 111**–**120.

(46) Aykin-Burns, N.; Ahmad, I. M.; Zhu, Y.; Oberley, L. W.; Spitz, D. R. *Biochem. J.* **2009**, *418*, 29–37.

(47) Liou, G.-Y.; Storz, P. *Free. Radic. Res.* **2010**, *44*, 479–496.

(48) Ahmad, I. M.; Aykin-Burns, N.; Sim, J. E.; Walsh, S. A.; Higashikubo, R.; Buettner, G. R.; Venkataraman, S.; Mackey, M. A.; Flanagan, S. W.; Oberley, L. W.; Spitz, D. R. *J. Biol. Chem.* **2005**, *280*, 4254–4263.

(49) Ganesh, V.; Baru, A. M.; Hesse, C.; Friedrich, C.; Glage, S.; Gohmert, M.; Jänke, C.; Sparwasser, T. *Infect. Immun.* **2014,** *82*, 1052**–**1063.

for TOC only